Journal of Systems Architecture 170 (2026) 103592

Contents lists available at ScienceDirect

Journal of Systems Architecture

journal homepage: www.elsevier.com/locate/sysarc

An FPGA-based accelerator design methodology for smart UAVs in precision agriculture: A case study☆

Gianluca Bellocchi [a,*], Daniel Madronal [b,1], Alessandro Capotondi [a], Francesca Palumbo [c], Andrea Marongiu [a]

[a] University of Modena and Reggio Emilia, Via Campi 213/B, Modena, 41125, Italy
[b] University of Sassari, Via Muroni 23, 07100, Sassari, Italy
[c] University of Cagliari, Via Marengo 3, Cagliari, 09123, Italy

ARTICLE INFO

Keywords:
UAV
Smart and precision agriculture
Companion computer
FPGA overlay
Accelerator-rich architecture

ABSTRACT

Smart and Precision Agriculture (SPA) methods and technologies, such as autonomous robots, AI/ML, sensors, and actuators, enhance farming productivity by automating the retrieval of environmental parameters and the decision-making process, while Fog- and Edge-based paradigms enable more informed and responsive practices. Unmanned Aerial Vehicles (UAVs) can autonomously inspect crops and promptly cooperate with terrestrial vehicles to perform treatments, as recently demonstrated by the EU-funded COMP4DRONES (C4D) research project, focused on the provisioning of innovative UAV technologies for civilian applications. Modern companion-equipped UAVs leverage Heterogeneous Systems-on-Chip (HeSoCs) to execute complex on-board tasks. HeSoCs generally combine a general-purpose, multi-core processor with a domain-specific accelerator-rich subsystem, massively integrating application-specific accelerators. Field Programmable Gate Arrays (FPGAs) are ideal fabrics to attain high performance and energy efficiency because of their massively parallel, deeply pipelined, non-Von-Neumann processing logic and custom memory hierarchies. Automated hardware-software co-design methodologies, e.g., FPGA overlays and toolflows, largely simplify the design phases, including the optimization of the accelerator interfaces, such as the merging of redundant components to reduce area usage. In this context, our contribution consists of a System-Level Design (SLD) methodology for the design of overlay-based UAV companion computers, including a modular and scalable accelerator-rich RISC-V HeSoC, a heterogeneous software stack, and an automation toolchain to generate and integrate application-specific accelerators into our overlay. Our results show three optimized overlay variants targeting an UAV-based system employed in a SPA context. Experimental results denote improvements in performance and area usage, up to 18.5% on a FPGA-based HeSoC with respect to traditional design flows.

1. Introduction

Smart and Precision Agriculture (SPA) is revolutionizing the agricultural industry with innovative methods to improve operational efficiency, farming yield, and crop health [1,2]. These approaches evolved with the advent of Internet of Things (IoT) solutions, which allowed farmers to monitor environmental parameters, perform analytics, and observe the status of farms and machinery, including soil and crop health, usage of agrochemicals, fertilizers, water and seeds, livestock conditions, temperature and energy consumption, and damage assessment caused by wildlife or natural forces [3–5]. This is achieved by employing cutting-edge technologies—including autonomous robots, AI/ML algorithms, and advanced sensors and actuators—to automate and enhance traditional human-centered farming activities [6–9].

Agriculture requires timely and targeted remedies to reduce resource waste and ensure land and plant productivity [10,11]. State-of-the-Art (SoA) computing paradigms—such as *Cloud*, *Fog* and *Edge*—are key to enabling SPA [12]. These offer significant advantages compared to traditional *Human-Centered* or *Offline* practices, which generally postpone the application of treatments and/or farmer intervention with a negative impact on the crops health status, costs, and productivity. *Offline* approaches involve initial on-field data collection

☆ This article is part of a Special issue entitled: 'CAES' published in Journal of Systems Architecture.

* Corresponding author at: University of Modena and Reggio Emilia, Via Giuseppe Campi 213/B, Modena, 41125, Italy.
E-mail addresses: gianluca.bellocchi@unimore.it (G. Bellocchi), dmadronalquin@uniss.it (D. Madronal), alessandro.capotondi@unimore.it (A. Capotondi), francesca.palumbo@unica.it (F. Palumbo), andrea.marongiu@unimore.it (A. Marongiu).
[1] Daniel Madronal is now with Airbus S.A.S.

https://doi.org/10.1016/j.sysarc.2025.103592
Received 1 March 2025; Received in revised form 31 July 2025; Accepted 26 September 2025
Available online 7 November 2025

and recordings, such as Light Detection and Ranging (LiDAR) point-clouds and multispectral images, followed by disjoint post-processing of raw measurements performed by offline servers that extract insightful parameters and classify activities [13–15]. However, this implies significant delays in the decision-making process and a negative impact on the plantation foreseeable future [16]. *Cloud*-based solutions process data online on dedicated servers. These retain major challenges, including privacy, scalability, high latency, network congestion, and Quality of Service (QoS) degradation when huge amounts of heterogeneous farming data are transmitted [11,17,18]. Moreover, some applications can suffer from the high energy consumption due to data transfer to and from the cloud [19]. *Fog*- and *Edge*-based solutions are similarly defined, as both bring cloud services and resources closer to the edge data sources [12]. Modern computing platforms make this practical, expediting data processing and enabling more informed, responsive practices by moving decision-making closer to the crops [20,21].

Autonomous Unmanned Aerial Vehicles (UAVs) will be pivotal in SPA activities, constituting reasonable human substitutes to examine the health status and growth evolution of the plantations, thus rapidly applying proper treatments [22]. The adoption of UAVs is mainly driven by the increased intelligence aboard and the advent of *companion-equipped drones* capable of executing complex tasks, e.g., real-time, data processing and analytics, or complex actuation [23–26]. Another driver is the value generated by collected data, sampled closer to the crops thus guaranteeing more informed decisions [27]. Moreover, UAVs are expected to extensively cooperate with other robots, including Unmanned Ground Vehicles (UGVs), for synergistic and collaborative aerial and ground operations, aimed at enhancing operational outcomes and providing greater flexibility in adapting to dynamic environments [28,29]. Given the heterogeneity of robots, the cooperation may happen in different ways to exploit their complementarities [30].

The EU's Common Agricultural Policy noted that greener farming practices will be fundamental to increase crop yield and meet the expected doubling of world food production by 2050, given no additional land will be available to meet these needs [31]. It is widely acknowledged that the future of farming relies on research, innovation, and capacity building in the agri-food sector, leveraging cutting-edge technologies, including advanced embedded systems, robotics, and digital platforms, which help to build a more sustainable and efficient food system. A recent example is provided by the EU-funded COMP4DRONES (C4D) research project[2] that focused on innovating UAV technologies for civilian applications [32]. One of the use-cases was specifically devoted to the improvement of the autonomous capabilities of UAV-based systems in the SPA context.[3] Meeting this requirement requires the ad-hoc re-design of the drone system and its components, where the *Flight Controller (FC)* is the most critical.

The FC is the UAV core component and many Commercial Off-The-Shelf (COTS) solutions are based on μ-controllers [33,34]. Modern UAVs integrate cutting-edge, *on-board companion computers* with SoA computing, memory, and network capabilities for advanced on-board, real-time data processing. These companion computers use embedded Heterogeneous Systems-on-Chip (HeSoCs), with many COTS solutions available [35]. These combine a general-purpose, multi-core processor with a domain-specific subsystem for specialized processing, such as a custom ASIC, GP-GPU, or *Field Programmable Gate Array (FPGA)*.

In particular, massively integrating application-specific accelerators in a single FPGA-based HeSoC—following a so-called *accelerator-rich paradigm*—offers unique opportunities for autonomous UAVs and SPA applications [36,37]. Indeed, such a companion computer can flexibly map and accelerate sophisticated workloads on its massively parallel, deeply pipelined, non-Von-Neumann processing logic and custom memory hierarchies, thus attaining high performance and low energy consumption, which is ideal for SPA applications [38,39]. However, heterogeneity hardens the hardware-software co-design process that is associated with bringing up the companion computer. Innovative approaches are thus required to mitigate design costs [40,41].

To this end, *FPGA overlays* are Hardware (HW) abstraction layers that simplify the mapping and scheduling of application tasks to the FPGA fabric [42]. *Toolflows* are crucial for optimizing accelerator communication and control interfaces, including I/O data ports and register files. In this context, Coarse-Grain Reconfigurable (CGR) accelerators represent a valuable option because they comprise low-overhead, decoupled, and inexpensive control interfaces. These features enable optimization strategies, including merging redundant accelerator parts. This optimization reduces area usage without additional overheads from complete or partial FPGA reconfiguration.

Under this premise, our contribution consists of a System-Level Design (SLD) methodology[4] for the design of overlay-based UAV companion computers, including:

- *On-board Overlay Compute Platform (OOCP)*, a modular and scalable accelerator-rich RISC-V HeSoC;
- *On-board Overlay Development Kit (OODK)*, a heterogeneous Software (SW) stack to ease heterogeneous application development;
- *Multi-Dataflow Composer (MDC)*, an automation toolchain to automatically generate and integrate CGR accelerators in OOCP.

We run the C4D use-case application on three variants of the OOCP architecture, which are deployed to a COTS FPGA-based HeSoC from the AMD Zynq Ultrascale+ (US+) family. Our experimental results show improvements in performance and area usage of up to 18.5% compared to traditional integration flows, thanks to the merging and optimization features of our proposed flow.

The manuscript is organized as follows. Section 2 describes background content, including the C4D project, the SPA use-case scenario, and UAV components. Section 3 discusses the related works, while Section 4 introduces the components of the SLD methodology—OOCP, OODK and MDC. Section 5 presents experimental results from three variants of our overlay-based UAV companion computer and assesses the methodology scalability for larger, more complex UAV systems. To demonstrate the broad applicability of the proposed approach, not limited to the SPA context, Section 6 describes additional projects enabled with the proposed approach.

2. Background

2.1. The COMP4DRONES project

The ECSEL JU project C4D—Framework of Key Enabling Technologies for Safe and Autonomous Drones—terminated in 2023 under the coordination of Indra and involvement of 50 partners. The Italian cluster included 12 partners and was led by the University of Sassari (UNISS), also involved in providing one of the assessment test cases for the C4D technologies. The main goal of the project was to offer a framework of key enabling technologies for the design and operation of drones, ranging from application to electronic components, realized as a tightly integrated multi-vendor and compositional embedded architecture solution, and a toolchain to assemble and safely operate drones [32]. The main idea of the assessment test case from the Italian cluster was to improve SPA technologies by providing more advanced observation and intervention methodologies through combined usage of a UAV and a UGV.

[2] https://cordis.europa.eu/project/id/826610

[3] https://www.youtube.com/watch?v=lNkCDg6HjiQ

[4] Our contributions—OOCP, OODK and MDC—are open-source, as parts of the C4D research project.

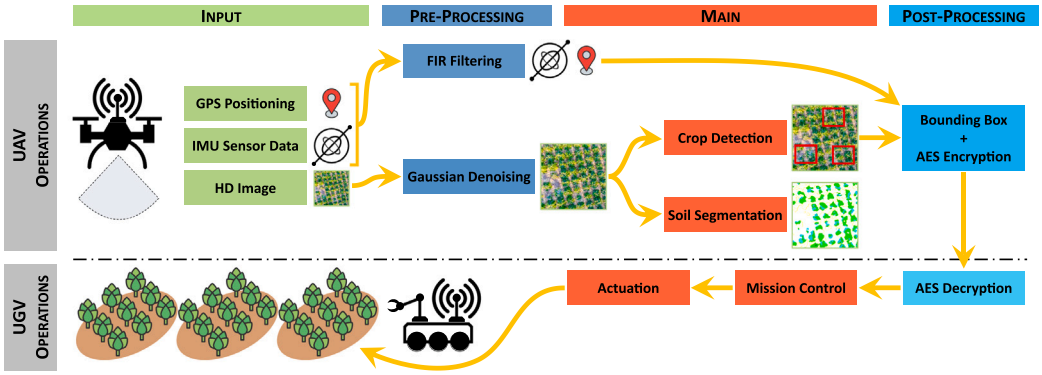

Fig. 1. Representation of the C4D use-case application scenario.

2.2. UAV for smart and precision agriculture

In the SPA context, UAVs may handle many tasks, including the mapping and detection of crops and plants [43–45], monitoring sessions and inspection operations [46–48], disease detection [49–51], and application of treatments [52,53]. Besides, flight-oriented data processing—including path planning, obstacle detection, and collision avoidance—is crucial for safe environment exploration [54–56].

The C4D SPA use-case scenario embodies a subset of the tasks above and, specifically, the autonomous detection and monitoring of artichoke crops. The final goal consists of preserving a healthy yield status by monitoring the crop health status and searching for potential anomalies during the UAV's aerial traversal over a preset plantation route. During the flight, the drone examines the plants and searches for crop discontinuities. Besides, the UAV collaborates with a UGV in a synergistic effort for plant monitoring and health and growth management. Closing the loop faster brings advantages in the agriculture context, which largely benefits from fast reactions to anomalies, at exact space and time. In general, both the UAV and the UGV act as mobile sensors: the drone acts as a *sentinel* ensuring rapid reconnaissance and online decisions, while the terrestrial rover acts as a *mobile actuator*, meant for detailed recognition, spot-on spraying of nutrients, water, and pesticides, and support in case of anomalies or abnormal circumstances. Besides, both extract and process complex plantation images to deduce relevant information and communicate over a trusted and secure medium, which is ensured with lightweight cryptographic modules for data-privacy, authentication and communication integrity.

Fig. 1 shows the C4D use-case application scenario, where the UAV and UGV collaborate synergistically. In this manuscript, we focus our attention on the portion of the use-case executed by the UAV, given the UGV employs the same hardware-software technologies. Hence, the processing pipeline implemented by the UAV consists of: (i) INPUT DATA ACQUISITION; (ii) PRE-PROCESSING; (iii) MAIN; and (iv) POST-PROCESSING.

The UAV initially samples both *visual and textual information*—including a 1440 × 900 HD image, IMU sensor data, and GPS position—and then forwards them to the companion computer, which initializes computing resources and starts executing the successive processing stages. As soon as the pre-processing phase starts, the field image is smoothed by applying *Gaussian Denoising* (`Conv`) to prune image noise for the subsequent processing steps, while IMU and GPS data encompass a *Finite Impulse Response* (`FIR`) filtering stage. Afterwards is the main processing phase, where *Crop Detection* and *Soil Segmentation* are executed. Crop detection is implemented by a *Convolutional Neural Network* (`CNN`) model for artichoke plant detection and classification through a customized Feature Pyramid Network CNN that works as a Single Shot Detector (SSD) [45]. Besides, image segmentation leverages at its heart a *Canny edge detector* (`Canny`) [57]. Finally, the post-processing stage packs textual data in a *Bounding BOX* (`BBOX`), which is subsequently encrypted with an *Advanced Encryption Standard* (`AES`) for trusted and secure communication toward the UGV.

2.3. UAV components

UAV systems include multi-rotor or fixed-wing frames, Electronic Speed Control (ESC) modules, and navigation systems that rely on sensors such as Inertial Measurement Units (IMUs), barometers, Global Navigation Satellite System (GNSS), and radio transmitters [35]. The FC is a crucial UAV component, with many COTS alternatives available [33]. It is typically based on μ-controllers and supports I/O interfaces for integrating sensors and payloads, e.g., cameras and LiDARs. The FC also handles functions such as flight control, navigation, data acquisition and processing, mission control, and actuation [34].

Modern UAVs couple the FC with cutting-edge, *onboard companion computers* to empower the drone system with advanced processing, memory, and network capabilities [16]. UAV companion computers typically adopt embedded HeSoCs, combining a general-purpose, multi-core processor with a domain-specific subsystem for advanced processing, such as a custom ASIC, GP-GPU, or FPGA.

We believe that FPGA-based HeSoCs offer significant advantages for the design of complex UAV stacks, such as on-the-fly deployment of computing tasks and embedded soft cores to simplify HW/SW application partitioning [38,66]. However, existing tools are not mature enough to reduce the design effort required to bring up a full-fledged FPGA-based companion computer integrating heterogeneous components and accelerators [40]. To this end, we propose an innovative SLD methodology based on a FPGA overlay to streamline design and optimization of accelerator-rich HeSoCs.

3. Related work

3.1. About the design of UAV companion computers for SPA applications

This section compares literature on companion-equipped drones for SPA applications, including our work. Our analysis focuses on works in which the UAV companion computer supports autonomous, informed decisions about crops, safe navigation in plantations, and communication with ground stations, other robots, and system components [26,28,35]. Table 1 summarizes the features of each approach.

UAV companion computers can be designed using homogeneous platforms, where SPA tasks are executed entirely on general-purpose CPUs. *Alsalam et al.* use the Odroid-U3+ to detect invasive weeds and implement a decision-making control loop [58]. The companion computer runs vision algorithms and controls the UAV flight height. Other components handle path planning, environment inspection, and herbicide application. Although the Odroid-U3+ integrates an ARM Cortex-A9 CPU and a Mali-400 GPU, it is only used to a limited extent and GPU acceleration is neither utilized nor discussed. Similarly, *Dai et al.* present a vision-based UAV system for spraying pesticides on fruit trees [59]. The system employs an Intel i5-6260 CPU to process images, handle flight control, and communicate with a ground station. In contrast, our UAV system communicates with a UGV in a synergistic effort

Table 1
Overview of UAV companion computers for SPA applications.

	Technology			Main SPA Task	
	Platform	**Type**	**Accelerator**	**Task**	**Algorithm**
Alsalam et al. [58]	Odroid-U3+	CPU	—	Weed detection	Vision
Dai et al. [59]	Intel i5-6260	CPU	—	Pesticides spraying	Vision
Horstrand et al. [60]	NVIDIA Jetson TK1	HeSoC	GPU	Crop monitoring	VI[a]
Saddik et al. [61]	Intel Cyclone V	HeSoC	FPGA	Crop monitoring	VI[a]
This Work	**AMD Zynq US+**	**HeSoC**	FPGA	**Crop detection, Soil Segmentation**	**CNN, Edge Detection**

[a] VI: Vegetation Index.

Table 2
Overview of SLD methodologies for FPGA-based HeSoCs.

	Accelerator					Overlay					
		Type				Host		Proxy Core[b]		Interconnect[c]	
	TI[a]	HLS	RTL	CGR	System-Level Integration	RV64	AArch64	RV32	MicroBlaze	Cluster-level	HeSoC-level
PYNQ [62]		✓			✓		✓		✓	–	STREAM
RobotCore [63]	✓	✓			✓		✓			–	STREAM
OpenESP [64]	✓	✓	✓		✓	✓				–	NOC
TaPaSCo [65]	✓	✓	✓		✓		✓			XBAR	XBAR
This Work	✔	✔	✔	✔	✔	✔	✔	✔	✔	**XBAR**	**XBAR**

[a] TI: Technology-Independent.
[b] Note that both OpenESP and TaPaSCo support RV32, but they do not exploit it as a proxy core, i.e., for tightly-coupled runtime management and optimization of accelerator scheduling, memory transfers and other pivotal platform tasks, as discussed in Section 4.1.
[c] Interconnects are classified as: (i) XBAR: Crossbar; (ii) NOC: Network-on-Chip; and (iii) STREAM: Based on a streaming protocol.

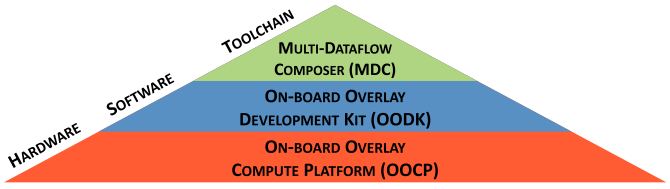

Fig. 2. System-level design stack.

to improve response time to anomalies in the plantation. Moreover, our approach and other works advocate heterogeneous platforms to increase intelligence aboard UAVs by combining CPUs and accelerators, such as FPGAs and GPUs, for more complex SPA tasks.

Horstrand et al. developed an autonomous UAV for hyperspectral measurements that provides vegetation indices for vineyard analysis [60]. The onboard computer includes an NVIDIA Jetson TK1 for autonomous flight control, data acquisition, processing, and communication with a ground station. However, the main limitations of GPUs are the non-extendable HW components, non-deterministic execution, and high power consumption, often exceeding the availability of resource-constrained autonomous robots [38,67].

To this end, FPGA-based HeSoCs are ideal solutions for UAV companion computers. *Saddik et al.* propose a vegetation monitoring system that accelerates GRVI and GLI indices using an Intel Cyclone V FPGA [61]. However, their Digital Signal Processor (DSP) utilization is low ($DSP_{\%,ref} = 6\%$), whereas previous works show benefits of highly-pipelined DSP datapaths in FPGA-based accelerators [68,69]. In contrast, our companion computer uses an accelerator-rich paradigm, where many application-specific accelerators are integrated to fully exploit the advantages of FPGA fabrics.

3.2. About SLD methodologies to simplify the design of FPGA-based HeSoCs

This section examines techniques to facilitate the design of FPGA-based HeSoCs. Table 2 summarizes characteristics of several industrial and academic approaches, including our own.

PYNQ is an open-source overlay design methodology that improves the usability of AMD HeSoC products [62]. It is particularly suitable for non-FPGA experts, as it greatly simplifies application development for embedded FPGA-based HeSoCs by offering support for Ubuntu Linux, Python, and Jupyter notebooks [70]. PYNQ overlays enable the deployment of accelerator-rich systems with support for dynamic partial reconfiguration [71]. However, beyond the provided examples, users must still undergo traditional platform development using the AMD Vivado Suite. In contrast, our SLD methodology fully automates the customization of accelerator-rich overlays. Users only require accelerator sources, e.g., designed with High Level Synthesis (HLS), and Python specification files to define: (i) how accelerators are interfaced and optimized (e.g., through datapath merging), as described in Section 4.2.2; and (ii) how accelerators are aggregated at the system-level along with their respective optimizations, as described in Section 4.3.

The PYNQ IP portfolio includes all AMD IPs, including: (i) a 64-bit ARM host processor, supporting legacy SW stacks; and (ii) a MicroBlaze soft core, providing a flexible and deterministic interface to a wide range of peripheral I/Os. In comparison, our OOCP features a broad portfolio of open-source IPs from the Parallel Ultra Low Power (PULP) Platform. Unlike PYNQ, our overlay is technology-independent, and our design flow can be extended to support FPGAs from different vendors.

Finally, the PYNQ soft core communicates with the host processor via shared memory, but supports only basic communication libraries [72]. To enable more complex interactions, users must implement their own communication SW, requiring development for two processors. However, complex UAV applications demand robust communication mechanisms between the host and the FPGA subsystem. Moreover, accelerator-rich systems require flexible control and optimization of data transfers and accelerator management. To address these needs, our OODK supports the OpenMP programming model, which simplifies the development of complex heterogeneous software. With this model, users write a single application that covers host and proxy core. The heterogeneous application begins execution on the host, while compute-intensive tasks are offloaded to the accelerator-rich subsystem using a dedicated computation offloading command [73]. Our FPGA overlay provides built-in support for flexible communication between the host and the accelerator-rich subsystem. This interaction

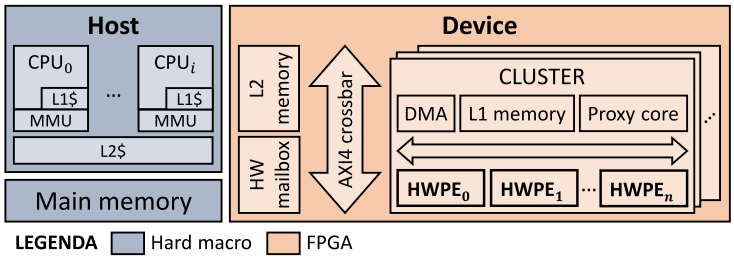

(a) HeSoC architecture deployed on Zynq US+ devices.

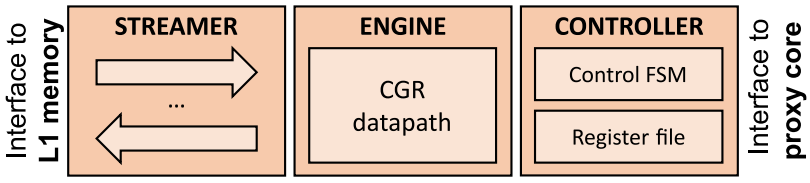

(b) HWPE-based wrapper.

Fig. 3. Overview of the OOCP components.

is managed by the proxy core, which acts as a man-in-the-middle to coordinate data movement and task execution across subsystems.

RobotCore targets Robot Operating System (ROS) 2 computational graphs for robotic applications [63]. The approach accelerates compute nodes and ROS 2 communication channels to reduce interactions with the host processor. RobotCore's FPGA subsystem is hardwired and less flexible than our programmable FPGA overlay.

OpenESP consists of a SLD framework for the seamless hardware-software integration of application-specific accelerators into HeSoCs [64]. Unlike our proposal, OpenESP uses the FPGA fabric as an emulation platform for ASIC prototyping and integrates coarse-grained accelerators that are loosely coupled with the processor. In contrast, our accelerator-rich overlay comprises numerous fine-grained accelerators, which are grouped into clusters and then integrated at the system-level—for example, to form more sophisticated accelerator-rich pipelines. Additionally, our approach differs from OpenESP in terms of SW support. While ESP interfaces accelerators using a Linux driver, OOCP connects accelerators directly within the heterogeneous application or through user-space libraries. This is enabled by our OODK, which provides full support for OpenMP [74].

Task Parallel System Composer (TaPaSCo) is an open-source methodology designed to simplify the development of accelerator-rich platforms, supporting many FPGA fabrics—from embedded devices to High Performance Computing (HPC) systems [65]. In TaPaSCo, HLS accelerators of the same type are grouped into homogeneous clusters. Heterogeneous platforms are then built by interconnecting different clusters. In contrast, our approach introduces heterogeneity directly at the level of OOCP clusters, which integrate heterogeneous, fine-grained accelerators. This architectural choice is fundamental to efficiently supporting accelerator-rich optimizations, including: (i) area-oriented techniques, such as datapath merging enabled by MDC; and (ii) performance-oriented strategies, such as the use of a proxy core for double-buffering and memory latency hiding, as discussed in Section 6.

TaPaSCo also supports RISC-V soft cores, used as processing elements for many-core platforms. Our proxy core is also RISC-V compliant but differs from the TaPaSCo soft core in intent. Indeed, the proxy core is a key enabler of high-performance, accelerator-rich platforms by orchestrating their many, co-existing tasks. This approach is flexible because it is SW-defined. This also includes the task scheduling of fine-grained accelerators, with automatic generation of SW libraries and Application Programming Interfaces (APIs). Furthermore, it is low-cost since the proxy core is tightly-coupled to the components of the OOCP cluster, including accelerators. This supervisory role of the proxy core does not limit the SW developer, who can still choose to deploy computation on the proxy core, as demonstrated in Section 6.2.

4. Methodology

This section describes our SLD methodology, shown in Fig. 2, which includes: (i) OOCP, an FPGA overlay based on a modular and scalable accelerator-rich RISC-V HeSoC; (ii) OODK, a heterogeneous SW stack to ease the development of heterogeneous applications; and (iii) MDC, an automation toolchain for automatic generation and integration of CGR accelerators in OOCP. We describe these components and the workflow enabling the design of overlay-based UAV companion computers.

4.1. Overlay architecture

Our FPGA overlay consists of two components: (i) *OOCP*, a modular and scalable accelerator-rich RISC-V HeSoC [75]; and (ii) *OODK*, a heterogeneous SW stack to streamline the development of heterogeneous applications. The overlay is based on the PULP Platform, an open and scalable hardware-software research and development platform for highly parallel, ultra-low-power architectures based on the open-source *RISC-V* Instruction Set Architecture (ISA) [76].

The OOCP architecture is a standard HeSoC with two independent subsystems—*host* and *device*—as shown in Fig. 3(a). The *host* is a Linux-capable multi-core application processor. If the target HeSoC fabric supports a physical host processor, then the latter can be leveraged with its HW/SW legacy. This is the case for the Zynq US+ family of devices, where an AArch64 application processor is integrated [77,78]. Alternatively, our architectural template supports the OpenHW Group CVA6 based on the RV64 ISA that can be implemented in FPGA [79].

The *device* subsystem consists of an accelerator-rich subsystem, including *clusters* of processing elements sharing a multi-banked SW-programmable L2 Scratchpad Memory (SPM) via a fully-connected AXI4 CrossBAR (XBAR). Host-device communication occurs via coarse-grained computational offloading, which leverages the off-chip main memory and a HW mailbox for synchronization.

Clusters integrate *accelerators*, a *proxy core*, L1 memory, and a SW-programmable Direct Memory Access (DMA) engine. L1 memory is implemented as a multi-banked Tightly-Coupled Data Memory (TCDM); L1 accesses occur through the cluster Low-Latency Interconnect (LIC).

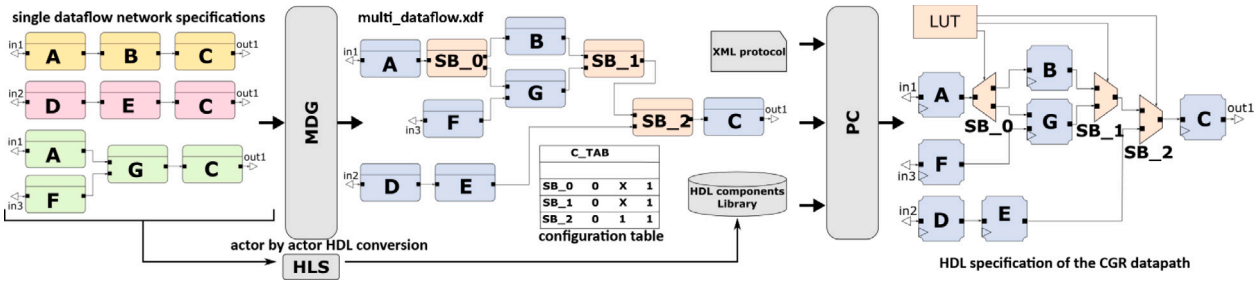

Fig. 4. MDC: From dataflow specification to the generation of a CGR datapath.

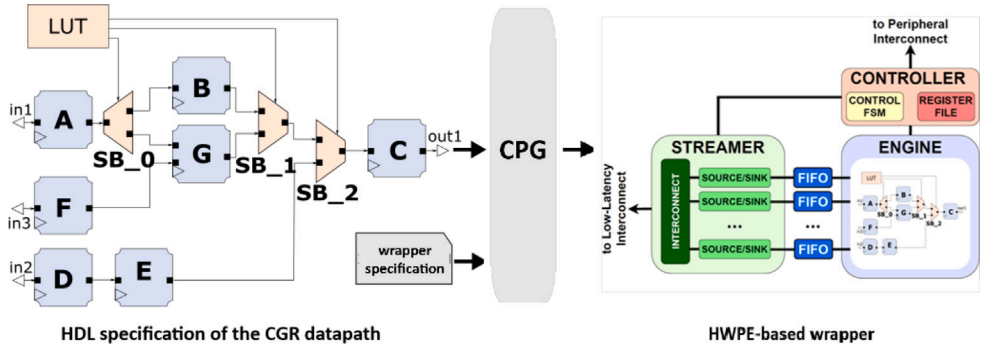

Fig. 5. MDC: From multi-dataflow specification to the generation of the HWPE wrapper.

The DMA supports efficient bi-directional 64-bit data transfers between the L2 and L1 memory hierarchies.

The *proxy core* is a pivotal component for tightly-coupled runtime management of cluster tasks, such as orchestration of accelerator tasks, DMA bandwidth monitoring, and control operations [80,81]. Moreover, it provides a flexible and customizable host-device interface. It consists of a low-cost soft core implementing the RV32 ISA that fetches instructions from L2 memory through its instruction cache [82,83]. This approach is more flexible than a dedicated Finite State Machine (FSM) and more scalable and tightly-coupled than costly host invocations.

Accelerators use Hardware Processing Engine (HWPE) interfaces for trustworthy and flexible communication between their datapaths and cluster components [84,85]. HWPE-based accelerators are integrated within the OOCP cluster and tightly-coupled to the L1 memory.

Fig. 3(b) shows the key modules of a HWPE wrapper: (i) an *engine*, implementing the accelerator datapath; (ii) a *streamer*, providing an I/O data interface to L1 memory; and (iii) a *controller*, for coarse-grained accelerator control and reconfiguration. The use of streaming interfaces decouples the CGR datapath from the outer system, providing benefits in terms of latency tolerance. Furthermore, the adoption of the HWPE wrapper increases MDC merging flexibility. Indeed, a typical concern with merging approaches is that they cannot usually handle the merging of kernels with different communication protocols due to incompatibilities at the I/O interface. With the adoption of HWPE, more diverse CGR datapaths can be merged into a single accelerator wrapper, which is then integrated into our accelerator-rich OOCP.

OODK is a heterogeneous SW stack supporting application developers. OODK supports the OpenMP programming model to ease the development of complex heterogeneous SW and a SoA LLVM-based heterogeneous compiler for the development of single-source, single-binary heterogeneous applications with OpenMP 4.5 offloading. The heterogeneous application always starts on the host processor and then critical tasks can be transparently offloaded to the accelerator-rich subsystem, simply by taking advantage of OpenMP pragmas.

4.2. Automatic generation of CGR accelerators

The design and integration of application-specific accelerators is accomplished by *MDC*, an open-source tool for generating CGR accelerators and integrating them into OOCP [86,87].

The typical MDC flow generates the following HW/SW components:

- *accelerator datapaths*, merging multiple functions into a single accelerator exploiting the principles of CGR reconfigurability;
- *accelerator wrappers*, providing communication and control interfaces for the interaction of CGR accelerator datapaths with other HW components that, in typical usage, serve as communication and control interfaces to the processing system;
- *accelerator drivers*, simplifying and abstracting the configuration and management of CGR accelerators within the wrapper.

4.2.1. CGR datapath generation

The generation of CGR datapaths is managed by the baseline MDC functionality, consisting of: (i) Multi-Dataflow Generator (MDG), a front-end that is responsible for datapath merging; and (ii) Platform Composer (PC), a back-end that translates a high-level merged dataflow model into an Hardware Description Language (HDL) specification.

The MDG requires a *dataflow specification*, which comprises a set of tasks (or functions) to be accelerated, defined as dataflow networks that are directed graphs connecting actors through First-In First-Out queues (FIFOs). In the example of Fig. 4, three tasks are represented in the top-left corner. The MDG block analyzes the input networks, locates the shared actors—A and C are shared in this specific case—and generates a *multi-dataflow network* combining all the functionalities. The combination is achieved by generating only one instance of each shared actor and including a set of switching boxes (SBoxes). These SBoxes enable the selection of the path that the data will follow when a specific functionality is selected for execution. To accomplish this, a *configuration table* containing the specific values to configure the SBoxes is also automatically generated.

Then, the PC derives the HDL specification of the CGR datapath from the multi-dataflow network, requiring: (i) an XML definition of

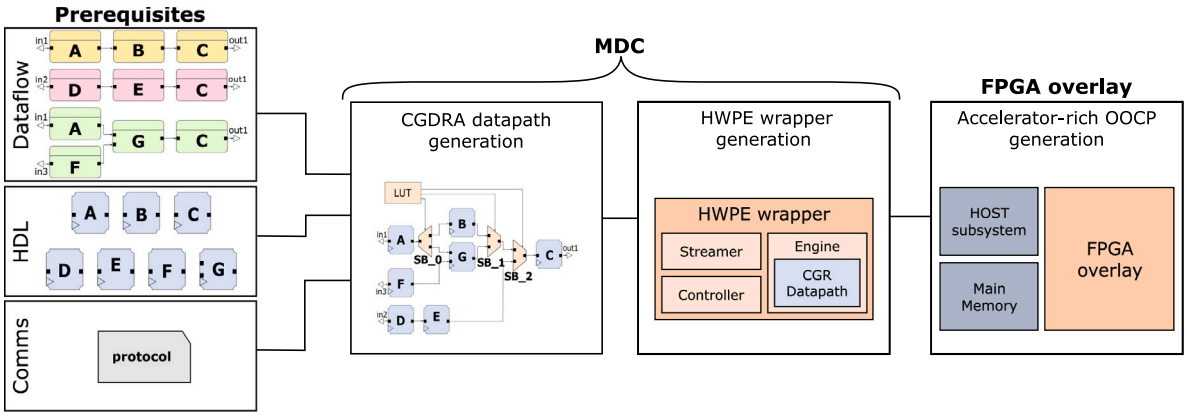

Fig. 6. SLD methodology to design full-fledged UAV companion computers based on an accelerator-rich FPGA overlay.

```
1  class oocp_specs:
2
3      def OOCP(self):
4          self.name      = Accelerator-rich platform
5          self.target    = FPGA fabric
6          self.l2_mem    = [Number of ports, Size]
7          return self
8
9      def cluster_0(self):
10         self.acc       = [Accelerator name, ...]
11         self.proxy     = [IP, Number of cores, ...]
12         self.dma       = [IP, Job queue size, ...]
13         self.l1_mem    = [Number of ports, Size]
14         return self
15
16     ...
17
18     def cluster_N(self)
19         ...
```

Listing 1: Example of OOCP specification.

actor communication protocols; and (ii) HDL actor descriptions (e.g., SystemVerilog, Verilog, or VHDL) from the *HDL components library*. These can be manually generated or automatically synthesized by leveraging HLS techniques such as Vitis HLS.

4.2.2. Automatic integration inside the FPGA overlay

An automatic procedure occurs for generating accelerator wrappers, which are necessary to integrate CGR accelerators within our OOCP.

To this end, MDC was extended to support the HWPE interface and ensure trustworthy and flexible communication between accelerators and OOCP components. HWPE-based accelerators are integrated inside the OOCP cluster and tightly-coupled to L1 memory.

The Co-Processor Generator (CPG) of MDC is shown in Fig. 5. CPG currently supports a novel feature that automatically generates HWPE-compliant wrappers. Through this feature, CPG has become capable of encapsulating the PC outcome—the CGR datapath of a reconfigurable accelerator—with the necessary glue logic for integrating it inside the OOCP cluster. Moreover, as part of this new feature, CPG also generates the necessary accelerator drivers to invoke the accelerator from the heterogeneous application developed via the OODK.

To this end, the tool requires a *wrapper specification* and the *CGR datapath specification*. The former describes the features of the integrated CGR datapath for customizing the HWPE streamer and controller.

Multiple CGR datapaths cannot run concurrently when merged in the same HWPE wrapper. However, switching functionality requires only a single clock cycle, as task selection occurs via the simple SW configuration of a HWPE register. Furthermore, the area usage of a multi-functional accelerator, where several tasks coexist in the same wrapper, is minimized thanks to the merging process of actors, I/O resources, and register files.

4.3. SLD methodology for UAV companion computers

The combination of our FPGA overlay with the MDC framework results in the SLD methodology shown in Fig. 6.

This workflow streamlines the design, optimization, and deployment of accelerator-rich UAV companion computers offering an abstract HW/SW co-design interface to improve ease-of-use and supporting datapath merging and automatic accelerator integration.

As prerequisites for using our SLD methodology, the user defines the application requirements, identifies the application tasks to accelerate, leverages the presented dataflow approach, and provides the input specifications as *dataflow networks*. Moreover, the user must provide a library of actors, described as *HDL specifications*, and the *communication protocol* specifying how they exchange data.

At this point, MDC automatically generates the *CGR datapaths*, merging the input tasks' specifications (as detailed in Section 4.2.1). Subsequently, MDC generates the HWPE wrappers and related drivers (as detailed in Section 4.2.2). Note that the merging process is completely under the user's control. The user selects the set of input dataflow specifications to be accelerated and passes them as input to MDC. In this work, we employ two strategies to select the set of tasks to be merged within the HWPE: (i) *application-aware*, which considers application task scheduling; and (ii) *specification-aware*, which considers the I/O characteristics of the input networks.

The integration of HWPE accelerators in OOCP and the design of the UAV companion computer are automated by a *toolchain* included in OODK. A *OOCP specification file* defines the key attributes of the accelerator-rich platform, including the characteristics of the OOCP and *cluster* fabrics and the distribution of accelerators across the platform.

Listing 1 shows an example of the `oocp_specs` class. The `OOCP` method (rows 3–7 of Listing 1) specifies the `name` and `target` for the FPGA fabric. The `l2_mem` parameter defines the L2 memory size and number of ports. The `cluster` method (rows 9–19 of Listing 1) specifies the attributes of the *cluster fabrics*. An arbitrary number of heterogeneous clusters can be defined, from `cluster_0` to `cluster_N`. The `acc` object specifies which accelerators to integrate within a *cluster*. Values assigned to `proxy`, `dma`, and `l1_mem` enable specialization of other *cluster* components. Additional parameters specify the number of *proxy cores* and allow flexible configuration of the DMA design. The L1 memory is similarly defined in terms of its size and number of ports. Based on these specifications, an accelerator-rich platform is automatically generated, with system-level integration of accelerators using the generated HWPE wrappers. Finally, an FPGA bitstream is built

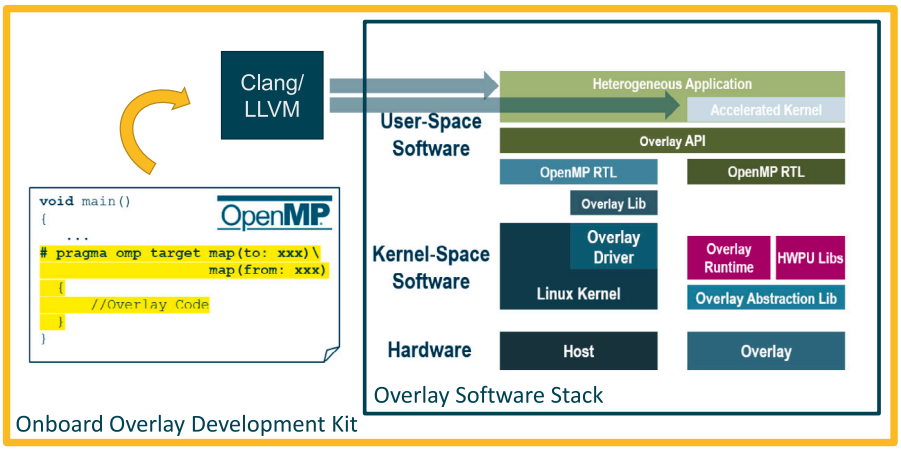

Fig. 7. OODK software compilation flow using OpenMP runtime API.

Table 3
FPGA resource availability of the AMD-Xilinx ZU9EG HeSoC fabric.

Resource type	Availability
Look-Up Tables (LUTs)	274 080
Flip Flops (FFs)	548 160
Block RAMs (BRAMs)	912
Digital Signal Processors (DSPs)	2520

using vendor-dependent tools (e.g., AMD Vivado Suite) to implement a specific *overlay* instance and complete the SLD design process.

Users can execute overlay application code using the high-level, established *OpenMP programming model*. Fig. 7 shows the compilation flow included in OODK. Users can offload portions of execution from the host processor to the overlay using the OpenMP accelerator model and target directives. Then, the accelerator APIs can be used to access accelerated functionalities. This high-level programming model proves to be much more flexible and agile compared to custom, low-level, vendor-specific models used in overlays like PYNQ and ESP.

5. Experimental evaluation

In this section, we leverage our SLD methodology to design a UAV companion computer for the C4D application scenario. First, we characterize the C4D use-case tasks, inspecting characteristics exploited at merge-time. Then, we propose three variants of our FPGA overlay, each integrating the C4D tasks, and profile performance and area usage to select the most suitable architecture for the SPA application.

5.1. Experimental setup

We implement OOCP on an AMD ZCU102 board, which integrates a Zynq US+ ZU9EG HeSoC. Table 3 reports the resource availability of the FPGA fabric, including: (i) Look-Up Tables (LUTs), i.e., reconfigurable digital circuits to implement combinational logic functions; (ii) Flip Flops (FFs), to save logical states, e.g., for processor and accelerator registers; (iii) Block RAMs (BRAMs), which can be cascaded to create large and fast memory arrays, e.g., SPMs and FIFOs; and (iv) DSPs (Digital Signal Processors), i.e., dedicated DSP slices.

We leverage, as a host processor, the physical ARM Cortex-A of the ZU9EG HeSoC that runs at f_{Host} = 1.2 GHz. We deploy the accelerator-rich subsystem to the FPGA fabric at f_{FPGA} = 100 MHz using the AMD Vivado Suite, including: (i) Vivado HLS v2018.2 to design the HW-accelerated use-case kernels; (ii) Vivado v2019.2 to build the FPGA bistream; and (iii) Petalinux v2019.2 to boot the OOCP.

The following sections include runtime performance measurements and FPGA resource utilization retrieved after the implementation phase.

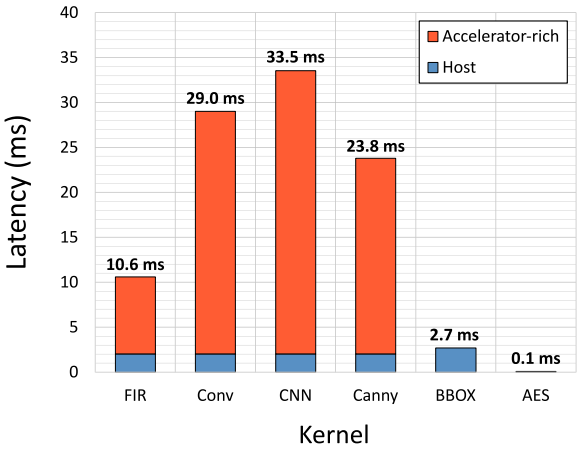

Fig. 8. Latency profiling of the use-case kernels.

5.2. Overview of the use-case SPA kernels

Acquiring details about the features of the SPA kernels is essential to guide the merge process, which is then influenced by different strategies, e.g., the *application task scheduling* and the characteristics of the *I/O accelerator interfaces*.

Table 4 summarizes the tasks composing the C4D SPA use-case scenario, along with a brief functional description. The Pre-Processing and Main phases are HW-accelerated in the accelerator-rich subsystem, while the Post-Processing is run in SW on the host processor. Notably, a companion computer targeting SPA applications is required to perform multiple accelerated functions during the mission. Moreover, it is worth pointing out that MDC supports different design approaches, which have been employed to develop these kernels. In particular, the CAPH language is used to develop the `Canny` [88], while HLS C/C++ is leveraged to design `FIR`, `Conv`, and `CNN`. Finally, the last column on the right shows the number of I/O interfaces for each kernel implementation. In the case of a HW accelerator, this consists of the actual I/O ports exposed at the interface of the CGR datapath, whereas for SW implementations, it consists of the number of I/O data arrays.

Fig. 8 shows the SPA kernel execution latency. Each bar represents a latency breakdown of execution on: (i) the *host*, including startup, allocation, and offloading; and (ii) the *accelerator-rich subsystem*, including the proxy core startup, DMA transfers, and accelerator execution.

Table 4
Overview of the C4D use-case kernels.

	Task	Kernel	Description	I/O
Pre-Processing	***Low-pass filter***	FIR	Fully-parallel systolic implementation, configurable with 64 or 128 coefficients.	1/1
	Blur	Conv	Dataflow implementation of a Gaussian Convolution with internal stages optimized in a pipeline manner.	1/1
Main	***Crop detection***	CNN	CNN Accelerator, configurable in different modes to accommodate variegated convolutional layers. The implementation is based on previous C4D partners work [45].	2/1
	Soil segmentation	Canny	Canny edge detector, based on a Sobel implementation [57].	2/1
Post-Processing	***Data annotation***	BBOX	Packing of textual metadata with image and IMU data.	3/1
	Data encryption	AES	AES data encryption.	1/1

Table 5
Overview of the adopted merge strategies.

Strategy	Implementation[a]
Baseline	$[FIR]_a$, $[Conv]_b$, $[CNN]_c$, $[Canny]_d$
Scenario-Agnostic	$[FIR + Conv]_a$, $[CNN + Canny]_b$
Scenario-Aware	$[FIR + Conv]_a$, $[CNN]_b$, $[Canny]_c$

[a] SPA kernels are either instantiated in dedicated wrappers $[kernel]_i$ or merged in a single wrapper $[\sum kernels]_i$.

5.3. Assembling an overlay-based UAV companion computer

We assemble *three variants* of our overlay-based UAV companion computer, leveraging the SLD methodology and the acquired information about the SPA kernels. Variants are designed to match the requirements of the C4D SPA use-case, described in Section 2, and *differ in the adopted merge strategies*, as shown in Table 5: (i) the Baseline instantiates a dedicated HWPE wrapper for each CGR datapath; (ii) the Scenario-Agnostic strategy groups CGR datapaths by the *number of input accelerator ports*, thus merging Conv and FIR, as well as CNN and Canny; and (iii) the Scenario-Aware strategy is driven by the *application task scheduling*, where the goal is to maximize the number of parallel tasks. CNN and Canny are instantiated in dedicated wrappers to run in parallel, since they have no mutual dependency and are very latency-expensive. Furthermore, Conv and FIR are merged, given the former has a dependency on both CNN and Canny; indeed, the execution of Canny can be hidden by running it in parallel with the other kernels.

The SW application starts on the host processor, which acquires sensor data and offloads the Pre-Processing and Main stages to the accelerator-rich subsystem. Once offloading completes, the RISC-V proxy core commands the DMA to move input data to local accelerator buffers. Data is divided into tiles due to limited L1 memory size. Once DMA transfers complete, accelerators are launched according to the execution profile of the C4D application. Fig. 9(a) shows a time diagram for the Scenario-Aware strategy, which guides accelerator optimization given the information about application task scheduling. The diagram also applies to the Baseline, as no merging constraints are applied to accelerators. In contrast, the Scenario-Agnostic strategy forces CNN and Canny to run sequentially, as they are merged in the same wrapper. The diagram includes color-coded features describing the number of accelerator I/O interfaces. BBOX and AES are not color-coded, as they are executed in SW on the host processor.

5.3.1. Latency

Fig. 9(b) shows the resulting execution latency for each variant. The Scenario-Aware approach terminates in 50.3 ms, while the Scenario-Agnostic strategy degrades by a factor of 13.7% due to the serialization

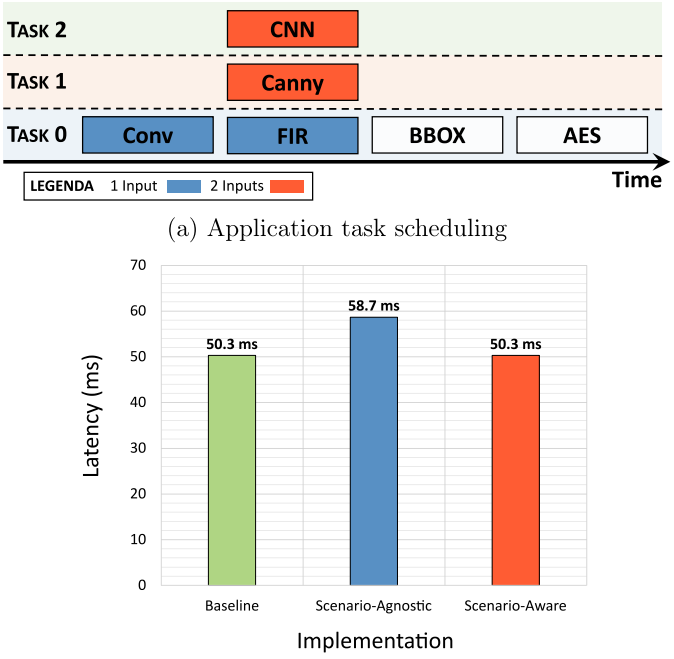

(a) Application task scheduling

(b) Execution latency

Fig. 9. Application task scheduling and execution latency concerning the three architectural variants of the overlay-based UAV companion computer.

of the CNN and Canny tasks. Additionally, the Baseline does not constrain kernels by merging their interfaces; thus, each can operate freely in parallel, following the application's profile. As a consequence, the latter performs as the Scenario-Aware approach.

5.3.2. Area usage

Table 6 shows the FPGA resource utilization of the Baseline variant, normalized to the resource availability of the ZU9EG HeSoC fabric. Values are organized according to three hierarchical levels: (i) *overlay-level*, referring to an OOCP instance with a single cluster, the host communication interface, i.e., the HW mailbox, and the L2 memory subsystem, accounting for resource usage of the AXI4 interconnect and the L2 SPM; (ii) *cluster-level*, with a RISC-V proxy core, DMA, L1 memory and the cumulative occupation of accelerator wrappers and datapaths; and (iii) *accelerator-level*, including specific information concerning the HWPE wrappers and CGR datapaths.

The main benefit of the merge process consists of the area savings originating from the sharing of the HWPE wrapper; thus, we expect

Table 6
FPGA utilization of the baseline C4D OOCP variant.

Overlay-level		LUT%	FF%	BRAM%	DSP%
	Host communication	2.0	0.7	0	0
	L2 memory	5.0	1.4	7.0	0
	Cluster	59.7	23.8	17.4	36.9
Cluster-level		**LUT%**	**FF%**	**BRAM%**	**DSP%**
	RISC-V soft core	8.6	1.5	9.6	0.4
	DMA	2.3	1.1	0	0
	L1 memory	11.1	3.7	2.9	0
	Accelerator wrappers	7.6	2.9	0	0
	Accelerator datapaths	30.3	14.7	4.9	36.6
Accelerator-level		**LUT%**	**FF%**	**BRAM%**	**DSP%**
FIR	Streamer	0.8	0.2	0	0
	Controller	0.4	0.4	0	0
	Datapath	8.6	8.5	0	5.1
Conv	Streamer	1.7	0.4	0	0
	Controller	0.9	0.4	0	0
	Datapath	1.6	0.8	2.4	0.5
CNN	Streamer	1.2	0.4	0	0
	Controller	0.6	0.4	0	0
	Datapath	10.5	1.6	0.1	30.5
Canny	Streamer	1.4	0.3	0	0
	Controller	0.6	0.4	0	0
	Datapath	9.6	3.8	2.4	0.5

Note: Normalized FPGA utilization (%) refers to the resource availability of the AMD-Xilinx ZU9EG HeSoC fabric used in our experiments.

Table 7
FPGA utilization of the C4D OOCP variants.

Overlay-level		LUT%	FF%	BRAM%	DSP%
	Baseline	66.7	25.9	24.4	36.9
	Scenario-Agnostic	54.0	21.5	24.4	36.9
	Scenario-Aware	55.7	22.3	24.4	36.9
Cluster-level		**LUT%**	**FF%**	**BRAM%**	**DSP%**
	Baseline	59.7	23.8	17.4	36.9
	Scenario-Agnostic	46.9	19.4	17.4	36.9
	Scenario-Aware	48.7	20.2	17.4	36.9
Accelerator-level		**LUT%**	**FF%**	**BRAM%**	**DSP%**
	Baseline	37.8	17.5	4.9	36.5
	Scenario-Agnostic	34.9	16.1	4.9	36.6
	Scenario-Aware	35.2	16.7	4.9	36.6

Note: Normalized FPGA utilization (%) refers to the resource availability of the AMD-Xilinx ZU9EG HeSoC fabric used in our experiments.

a reduction in their area usage with greater use of the optimization. With a reduction in the number of wrappers, fewer L1 memory ports are required, thus positively affecting the occupation of the cluster LIC (combined with the L1 memory). Thus, LUT usage would decrease by up to $\Delta_{LUT,max} = -18.7\%$, consisting of about 28% of the Baseline overlay. Furthermore, FF usage is expected to decrease by up to $\Delta_{FF,max} = -6.6\%$, representing 26% of the Baseline overlay.

Table 7 shows the occupation results of each merging strategy to confirm these conjectures. Indeed, at the overlay-level, we observe a maximum decrement in resource occupation of $\Delta_{LUT} = -12.7\%$ and $\Delta_{FF} = -4.4\%$ corresponding to the Scenario-Agnostic approach. No variation applies to BRAMs and DSPs because the merge does not apply to the CGR datapaths or other overlay components that use those macros. Zooming in at the cluster-level, the same decrement is found, as the merge only influences the cluster components: the accelerator wrappers and the cluster LIC.

5.3.3. Performance and area trade-off

We investigate the three variants more deeply, examining aggregated trade-offs based on performance and FPGA resource utilization—LUT and FF usage. The implementation that best responds to trade-offs is determined by the larger value of the aggregated metric, which is normalized to the results of the Scenario-Aware strategy.

Fig. 10(a) and 10(b) show the performance and LUT occupation trade-off. The Scenario-Aware strategy improves over the Baseline OOCP by 16.5% and 18.5% at overlay- and cluster-levels. Although the Scenario-Agnostic performs worse than the Baseline, as described in Section 5.3.1, it shows better trade-offs by 5.0% and 7.4%. Moreover, the trade-off is more impacted by merging when zooming into the cluster, since the merge applies only to cluster components.

Figs. 10(c) and 10(d) show the performance and FF occupation trade-off. In this case, the Scenario-Aware approach improves over the Baseline OOCP by 14.0% and 15.2% at the overlay- and cluster-levels, while the Scenario-Agnostic improves by factors of 2.7% and 7.3%.

5.3.4. Scalability analysis

This experiment assesses the methodology scalability for larger UAV companion computers. We assume $N_{acc} = 16$ accelerators is sufficient to gain meaningful insights, as commercial HeSoCs tend to integrate low-tens of accelerators into shared-memory clusters [89–91]. Further scaling introduces challenges due to single-cluster limitations, such as contention and interference among shared components. A widely adopted solution is to aggregate accelerators into multi-cluster, accelerator-rich architectures. This approach reduces pressure on shared cluster components but incurs additional FPGA resource overhead, thereby necessitating investigation into the overlay scalability.

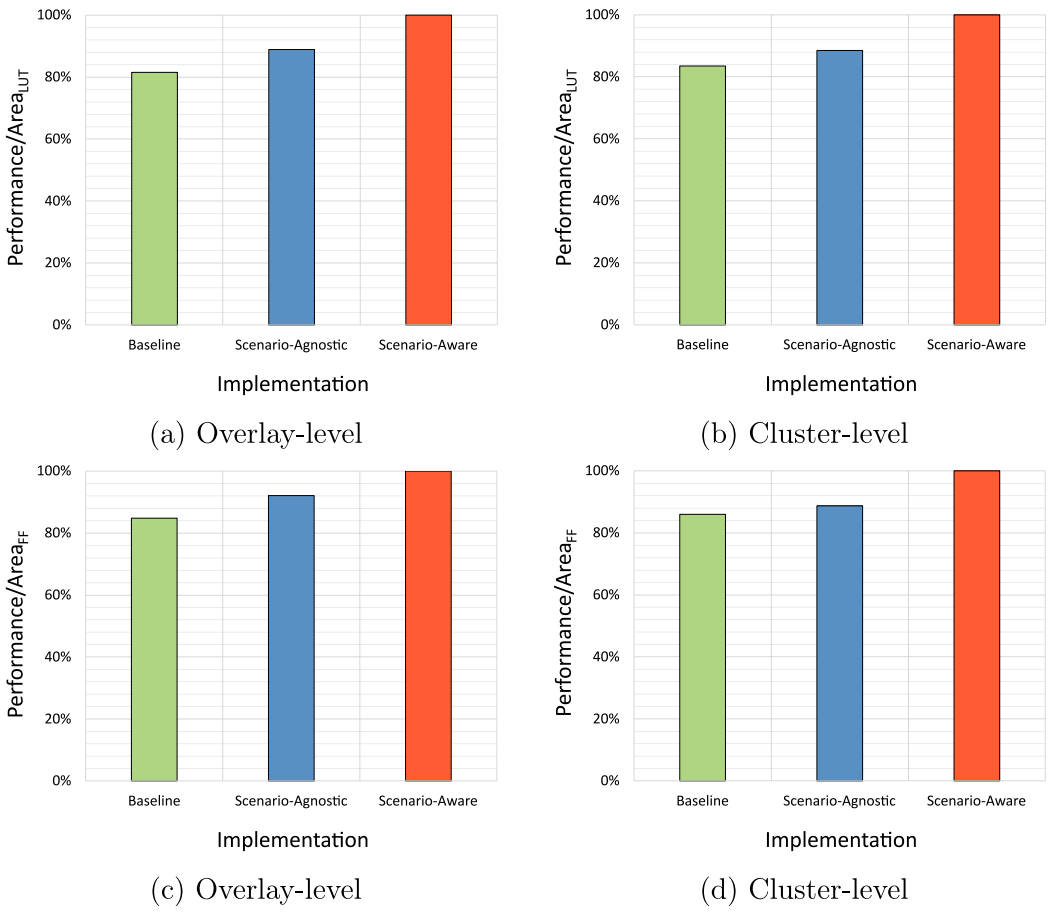

Fig. 10. Trade-off between performance and FPGA resource utilization (LUT, FF).

To this end, we assemble five multi-cluster OOCP variants using our SLD methodology. Each variant includes N_{acc} accelerators, evenly distributed across up to 16 clusters. Additionally, we scale the L2 memory subsystem according to the number of clusters (N_{CL}); thus, we expose more memory ports and banks (N_{L2P}), enabling each cluster to access data and instructions independently. We scale N_{CL} and N_{L2P} simultaneously. The largest variant is 16CL, with each accelerator integrated into a dedicated cluster.

Table 8 shows absolute and relative experimental values. Relative values are normalized to the value of the 1CL variant to gain insights into multi-cluster scalability relative to a baseline, i.e., the single-cluster instance of our FPGA overlay. These values represent overlay implementation costs, excluding application-specific accelerator datapath and wrapper. BRAMs and DSPs scale linearly with N_{CL} due to additional L2 memory ports and proxy cores, i.e., 1 per cluster. In contrast, LUTs and FFs increase by about 10× with 16CL. Re-aggregating accelerators into multiple clusters reduces the cost per cluster, as fewer LIC accelerator ports are exposed, and some components, such as those dedicated to host communication, are not replicated when scaling, as previously shown in Table 6. However, a critical contributor to LUTs and FFs is the fully-connected AXI4 XBAR at the HeSoC-level. To this end, it is worth noting that we are working on extending the IP portfolio of our FPGA overlay with a Network-on-Chip (NoC) architecture to enhance the scaling capability of our methodology [92].

The preceding discussion provides insights into the implementation cost of an empty overlay, i.e., the "skeleton" of a multi-cluster, accelerator-rich HeSoC. We conclude by presenting an additional analysis that integrates the previous findings. Fig. 11 shows five example accelerators from the literature, including: (i) `DPU-B512`, an AMD Deep Learning Processor Unit (DPU) for Convolutional Neural Network (CNN) acceleration (B512 configuration) [93]; (ii) `AD-Lane`, a Computer Vision (CV) accelerator-rich pipeline for lane detection [94]; (iii) `AD-PF`, a Particle Filter (PF) to accelerate the localization component in a perception-plan-act Autonomous Driving (AD) stack [80]; (iv) `DPU-B4096`, an AMD DPU for CNN acceleration (B4096 configuration) [93]; and (v) **C4D-UAV**, our UAV companion computer for SPA applications implementing the Scenario-Aware strategy, described in Section 5.3. As a side note, more details concerning `AD-Lane` and `AD-PF` can be found in Section 6.

We evaluate the FPGA resource usage of each accelerator, normalized to the resource consumption of a single-cluster overlay.[5] This normalization enables a meaningful comparison of the FPGA resources required to implement real-world accelerators, including those from our accelerator-rich use-case scenario. The results intuitively reveal how efficiently resources are utilized: higher normalized values suggest more effective use of FPGA resources by the accelerator itself, while lower values imply greater overhead introduced by the overlay. However, it is important to emphasize that the overlay cluster should not be regarded as overhead per se. As discussed in Section 4.1, the cluster and its components are fundamental to building high-performance, accelerator-rich systems [36,37,95].

The results are presented using two vertical axes: the left axis shows LUT, FF, and BRAM utilization, while the right axis displays DSP usage. This dual-axis format improves readability, as the normalized values for these two groups of FPGA resources differ significantly in scale.

[5] A normalized value of 1.0 indicates that the accelerator uses the same amount of resources as the overlay; a value of 2.0 indicates twice the resource usage.

Table 8
Scalability analysis of the proposed FPGA overlay.

			LUT		FF		BRAM		DSP	
Overlay[a]	N_{CL}[b]	N_{L2_P}[c]	Abs[d]	Rel[e]	Abs	Rel	Abs	Rel	Abs	Rel
1Cl	1	1	89495	1.0	56395	1.0	184	1.0	9	1.0
2Cl	2	2	129342	1.45	98755	1.75	368	2.0	18	2.0
4Cl	4	4	222986	2.49	173135	3.07	736	4.0	36	4.0
8Cl	8	8	407514	4.55	314644	5.58	1472	8.0	72	8.0
16Cl	16	16	899865	10.05	590244	10.47	2944	16.0	144	16.0

[a] **Overlay**: Multi-cluster variants of the FPGA overlay.
[b] N_{CL}: Number of clusters.
[c] N_{L2_P}: Number of L2 memory ports.
[d] **Abs**: Absolute FPGA utilization.
[e] **Rel**: Relative FPGA utilization normalized to the absolute value of the 1Cl variant.

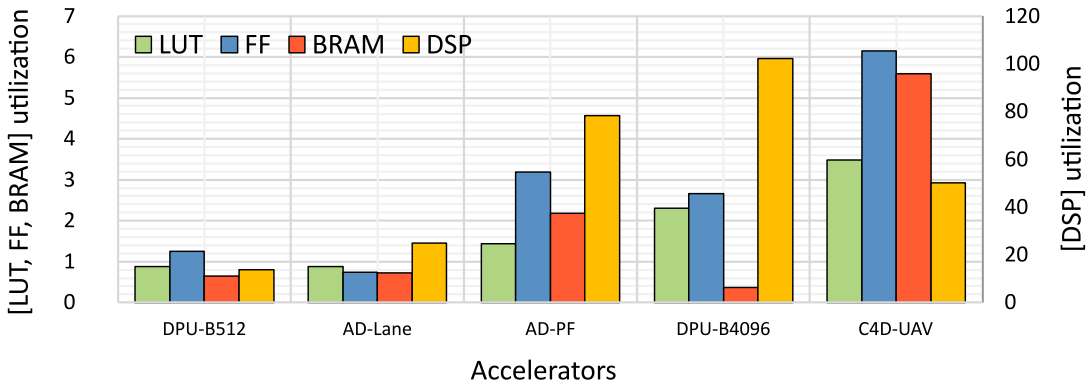

Fig. 11. Examples of five accelerators from the literature, including: (i) `DPU-B512`, AMD DPU for CNN acceleration (B512 configuration) [93]; (ii) `AD-Lane`, CV accelerator-rich pipeline for lane detection [94]; (iii) `AD-PF`, PF to accelerate the localization component in a perception-plan-act AD stack [80]; (iv) `DPU-B4096`, AMD DPU for CNN acceleration (B4096 configuration) [93]; and (v) **C4D-UAV**, our accelerator-rich use-case. We analyze the FPGA resource usage of each accelerator, normalized to the resource consumption of a single-cluster overlay. Results are presented using two vertical axes: the *left axis* for LUTs, FFs, and BRAMs, and the *right axis* for DSPs.

It can be observed that for simple accelerators and pipelines such as AccDpuSmall and `AD-Lane`, the resource overhead introduced by the overlay is comparable and, in some cases, equivalent ($\approx 1\times$) to that of individual application-specific datapaths. This indicates that even in fine-grained scenarios, the cost associated with the overlay is not prohibitive and does not hinder its practical adoption.

More notably, in more complex configurations—such as `DPU-B4096`, `AD-PF`, and our **C4D-UAV**—the resource impact of the overlay becomes virtually negligible, with overheads ranging from slightly above $2\times$ to up to $6\times$ across all resource classes.

6. Discussion

In this section, we discuss further application scenarios enabled with our SLD methodology. These demonstrate its broader applicability, not limited to the SPA context. In particular, we focus on two AD use-cases concerning F1TENTH autonomous racing competitions [96].

F1TENTH is an open-source platform for autonomous racing with 1:10 scaled cars for safe and rapid experimentation of AD systems and algorithms. Given their small size, these cars mount very constrained computing platforms, thus mandating deep AD stack optimization to attain target Key Performance Indicators (KPIs), e.g., performance, area, and energy consumption.

These examples prove that our FPGA overlay, with its automation flow and proxy core support, simplifies the integration of application-specific accelerators and the HW/SW partitioning and optimization of complex applications deployed to FPGA-based HeSoCs.

6.1. AD-Lane: A computer vision pipeline for lane detection

The first use-case concerns `AD-Lane`, a CV pipeline for *lane detection* that autonomously identifies road lane markings and guarantees that the AD system follows the correct path [94].

Using the same methodology applied to the UAV companion computer, we examine the pipeline stages and accelerate the most critical stages with the AMD Vitis Vision HLS Library [97]. Non-accelerated tasks are executed in SW, given the limited capability of the AMD Kria KV260 board. We integrate `AD-Lane` using our FPGA overlay and explore the benefits of the following HW/SW optimizations: (i) the *proxy core* improves the performance of accelerators with many input parameters with respect to looser and costly interactions with the host processor; (ii) the *L1 memory* benefits memory-bound stages, given that a tightly-coupled accelerator SPM provides lower access latency and better predictability compared to the off-chip main memory; and (iii) *pipelining* the memory and compute phases according to a double buffering memory scheme, orchestrated by the proxy core, improves overall performance compared to sequential execution. Ultimately, we achieve a $22\times$ speedup, compared to a SW-only implementation.

6.2. AD-PF: Real-time LiDAR-based autonomous localization

The second use-case concerns `AD-PF`, a typical perception-plan-act AD stack, where we accelerate the localization component, a Monte-Carlo method named *PF* [80]. We leverage the PF to localize the car in a pre-built map using perception data from a LiDAR sensor, while the optimal car trajectory is computed offline, and the control loop is closed with a pure pursuit algorithm. Since the application concerns racing vehicles, HW/SW optimizations aim to maximize average speed

on single laps and peak speed in head-to-head situations. Experiments are conducted on real-life race tracks with two boards (AMD ZCU102, Avnet Ultra96). We examine the impact of individual pipeline stages and accelerate the most critical one, i.e., the *Ray Marching (RM)* stage taking up to 90% of the overall PF execution. Hence, we design a *Ray Marching Engine* (RME) with HLS that achieves a 2.5× speedup compared to a pure SW implementation. Performance is further improved by $2-3\times$ with the integration of the RME within our FPGA overlay and exploiting the *proxy core* to optimize memory transfers between HeSoC subsystems—host and device.

7. Conclusions

In this work, we have contributed an innovative SLD methodology for the design of overlay-based UAV companion computers. The methodology tackles the challenge of facilitating the assembly of full-fledged UAV companion computers targeting *SPA* applications, as is one of the use-case scenarios of the EU-funded C4D research project.

The workflow includes a modular and scalable accelerator-rich RISC-V HeSoC, a heterogeneous SW stack to simplify heterogeneous application development, and a toolflow to automatically generate and integrate application-specific CGR accelerators in the FPGA overlay.

We run the C4D use-case application on three variants of the OOCP architecture, which are deployed to a COTS FPGA-based HeSoC from the AMD Zynq US+ family. Results demonstrate up to 18.5% improvements in performance and area usage.

The proposed methodology not only demonstrates the integration capabilities of accelerator-rich systems but also paves the way for new research directions. First, the architectural template can be extended with additional IPs to achieve better scalability in increasingly accelerator-dense environments. In this regard, we are working on expanding the IP portfolio of our overlay with FlooNoC[6] [92]. A second promising direction is to investigate and integrate automated design space exploration methods for optimal selection of integration and merging strategies for accelerators.

CRediT authorship contribution statement

Gianluca Bellocchi: Writing – review & editing, Writing – original draft, Validation, Software, Methodology, Investigation, Formal analysis, Data curation. **Daniel Madronal:** Writing – review & editing, Writing – original draft, Supervision, Methodology, Data curation. **Alessandro Capotondi:** Writing – review & editing, Writing – original draft, Supervision, Conceptualization. **Francesca Palumbo:** Writing – review & editing, Writing – original draft, Supervision, Conceptualization. **Andrea Marongiu:** Writing – review & editing, Writing – original draft, Supervision, Conceptualization.

Declaration of generative AI in scientific writing

This document is to declare that the authors have not leveraged the use of generative AI and AI-assisted technologies in scientific writing upon submission of the paper.

Declaration of competing interest

The authors declare the following financial interests/personal relationships which may be considered as potential competing interests: Andrea Marongiu reports financial support was provided by European Union. If there are other authors, they declare that they have no known competing financial interests or personal relationships that could have appeared to influence the work reported in this paper.

[6] https://github.com/pulp-platform/FlooNoC

Acknowledgments

This work was supported by the EU commission under the ECSEL-JU COMP4DRONES project (No. 826610) and the NextGenerationEU Programme within the Plan "PNRR - Missione 4 "Istruzione e Ricerca" - Componente C2 Investimento 1.1 "Fondo per il Programma Nazionale di Ricerca e Progetti di Rilevante Interesse Nazionale (PRIN)" by the Italian Ministry of University and Research (MUR)", project title: "Simplifying Predictable and energy-efficient Acceleration from Cloud to Edge (SPACE)", project code: 202254AM7H, CUP: E53D23007810006, MUR D.D. financing decree n. 959, 30th June 2023.

References

[1] R. Gebbers, V.I. Adamchuk, Precision agriculture and food security, Science 327 (5967) (2010) 828–831.
[2] R. Bongiovanni, J. Lowenberg-DeBoer, Precision agriculture and sustainability, Precis. Agric. 5 (2004) 359–387.
[3] A. Monteiro, S. Santos, P. Gonçalves, Precision agriculture for crop and livestock farming—Brief review, Animals 11 (8) (2021) 2345.
[4] H. Azadi, S.M. Moghaddam, S. Burkart, H. Mahmoudi, S. Van Passel, A. Kurban, D. Lopez-Carr, Rethinking resilient agriculture: From climate-smart agriculture to vulnerable-smart agriculture, J. Clean. Prod. 319 (2021) 128602.
[5] N. Ahmed, D. De, I. Hussain, Internet of Things (IoT) for smart precision agriculture and farming in rural areas, IEEE Internet Things J. 5 (6) (2018) 4890–4899.
[6] T.A. Shaikh, T. Rasool, F.R. Lone, Towards leveraging the role of machine learning and artificial intelligence in precision agriculture and smart farming, Comput. Electron. Agric. 198 (2022) 107119.
[7] H. Yin, Y. Cao, B. Marelli, X. Zeng, A.J. Mason, C. Cao, Soil sensors and plant wearables for smart and precision agriculture, Adv. Mater. 33 (20) (2021) 2007764.
[8] D. Xie, L. Chen, L. Liu, L. Chen, H. Wang, Actuators and sensors for application in agricultural robots: A review, Machines 10 (10) (2022) 913.
[9] P.K.R. Maddikunta, S. Hakak, M. Alazab, S. Bhattacharya, T.R. Gadekallu, W.Z. Khan, Q.-V. Pham, Unmanned aerial vehicles in smart agriculture: Applications, requirements, and challenges, IEEE Sensors J. 21 (16) (2021) 17608–17619.
[10] E. Karunathilake, A.T. Le, S. Heo, Y.S. Chung, S. Mansoor, The path to smart farming: Innovations and opportunities in precision agriculture, Agriculture 13 (8) (2023) 1593.
[11] J. Liu, J. Xiang, Y. Jin, R. Liu, J. Yan, L. Wang, Boost precision agriculture with unmanned aerial vehicle remote sensing and edge intelligence: A survey, Remote. Sens. 13 (21) (2021) 4387.
[12] Y. Kalyani, R. Collier, A systematic survey on the role of cloud, fog, and edge computing combination in smart agriculture, Sensors 21 (17) (2021) 5922.
[13] M.P. Christiansen, M.S. Laursen, R.N. Jørgensen, S. Skovsen, R. Gislum, Designing and testing a UAV mapping system for agricultural field surveying, Sensors 17 (12) (2017) 2703.
[14] P. Katsigiannis, L. Misopolinos, V. Liakopoulos, T.K. Alexandridis, G. Zalidis, An autonomous multi-sensor UAV system for reduced-input precision agriculture applications, in: 2016 24th Mediterranean Conference on Control and Automation, MED, IEEE, 2016, pp. 60–64.
[15] J. Primicerio, S.F. Di Gennaro, E. Fiorillo, L. Genesio, E. Lugato, A. Matese, F.P. Vaccari, A flexible unmanned aerial vehicle for precision agriculture, Precis. Agric. 13 (4) (2012) 517–523.
[16] D. Madroñal, F. Palumbo, A. Capotondi, A. Marongiu, Unmanned vehicles in smart farming: A survey and a glance at future horizons, in: Proceedings of the 2021 Drone Systems Engineering and Rapid Simulation and Performance Evaluation: Methods and Tools Proceedings, 2021, pp. 1–8.
[17] Y. Liu, X. Ma, L. Shu, G.P. Hancke, A.M. Abu-Mahfouz, From industry 4.0 to agriculture 4.0: Current status, enabling technologies, and research challenges, IEEE Trans. Ind. Inform. 17 (6) (2020) 4322–4334.
[18] J. Chen, X. Ran, Deep learning with edge computing: A review, Proc. IEEE 107 (8) (2019) 1655–1674.
[19] H.A. Alharbi, M. Aldossary, Energy-efficient edge-fog-cloud architecture for IoT-based smart agriculture environment, Ieee Access 9 (2021) 110480–110492.
[20] J. Su, X. Zhu, S. Li, W.-H. Chen, AI meets UAVs: A survey on AI empowered UAV perception systems for precision agriculture, Neurocomputing 518 (2023) 242–270.
[21] P.P. Ray, A review on TinyML: State-of-the-art and prospects, J. King Saud Univ.-Comput. Inf. Sci. 34 (4) (2022) 1595–1623.
[22] P. Radoglou-Grammatikis, P. Sarigiannidis, T. Lagkas, I. Moscholios, A compilation of UAV applications for precision agriculture, Comput. Netw. 172 (2020) 107148.
[23] L. Valente, A. Nadalini, A. Veeran, M. Sinigaglia, B. Sa, N. Wistoff, Y. Tortorella, S. Benatti, R. Psiakis, A. Kulmala, et al., A heterogeneous RISC-V based SoC for secure nano-UAV navigation, 2024, arXiv preprint arXiv:2401.03531.

[24] A. Di Mauro, M. Scherer, D. Rossi, L. Benini, Kraken: A direct event/frame-based multi-sensor fusion soc for ultra-efficient visual processing in nano-uavs, 2022, arXiv preprint arXiv:2209.01065.

[25] P. Foehn, E. Kaufmann, A. Romero, R. Penicka, S. Sun, L. Bauersfeld, T. Laengle, G. Cioffi, Y. Song, A. Loquercio, et al., Agilicious: Open-source and open-hardware agile quadrotor for vision-based flight, Sci. Robot. 7 (67) (2022) eabl6259.

[26] A. Douklias, L. Karagiannidis, F. Misichroni, A. Amditis, Design and implementation of a UAV-based airborne computing platform for computer vision and machine learning applications, Sensors 22 (5) (2022) 2049.

[27] D.C. Tsouros, S. Bibi, P.G. Sarigiannidis, A review on UAV-based applications for precision agriculture, Information 10 (11) (2019) 349.

[28] I. Munasinghe, A. Perera, R.C. Deo, A comprehensive review of uav-ugv collaboration: Advancements and challenges, J. Sens. Actuator Netw. 13 (6) (2024) 81.

[29] M. Mammarella, L. Comba, A. Biglia, F. Dabbene, P. Gay, Cooperation of unmanned systems for agricultural applications: A case study in a vineyard, Biosyst. Eng. 223 (2022) 81–102.

[30] J. Chen, X. Zhang, B. Xin, H. Fang, Coordination between unmanned aerial and ground vehicles: A taxonomy and optimization perspective, IEEE Trans. Cybern. 46 (4) (2015) 959–972.

[31] S.J. Undertaking, et al., European drones outlook study: unlocking the value for Europe, 2017.

[32] R. Nouacer, M. Hussein, H. Espinoza, Y. Ouhammou, M. Ladeira, R. Castiñeira, Towards a framework of key technologies for drones, Microprocess. Microsyst. 77 (2020) 103142.

[33] N. Aliane, A survey of open-source UAV autopilots, Electronics 13 (23) (2024) 4785.

[34] E. Ebeid, M. Skriver, J. Jin, A survey on open-source flight control platforms of unmanned aerial vehicle, in: 2017 Euromicro Conference on Digital System Design, Dsd, IEEE, 2017, pp. 396–402.

[35] A. Wilson, A. Kumar, A. Jha, L.R. Cenkeramaddi, Embedded sensors, communication technologies, computing platforms and machine learning for UAVs: A review, IEEE Sensors J. 22 (3) (2021) 1807–1826.

[36] J. Cong, M.A. Ghodrat, M. Gill, B. Grigorian, K. Gururaj, G. Reinman, Accelerator-rich architectures: Opportunities and progresses, in: 2014 51st ACM/EDAC/IEEE Design Automation Conference, DAC, IEEE, 2014, pp. 1–6.

[37] M.J. Lyons, M. Hempstead, G.-Y. Wei, D. Brooks, The accelerator store: A shared memory framework for accelerator-based systems, ACM Trans. Archit. Code Optim. (TACO) 8 (4) (2012) 1–22.

[38] Z. Wan, A. Lele, B. Yu, S. Liu, Y. Wang, V.J. Reddi, C. Hao, A. Raychowdhury, Robotic computing on FPGAs: Current progress, research challenges, and opportunities, 2022, arXiv preprint arXiv:2205.07149.

[39] Y. Chi, W. Qiao, A. Sohrabizadeh, J. Wang, J. Cong, Democratizing domain-specific computing, Commun. ACM 66 (1) (2022) 74–85.

[40] L.P. Carloni, The case for embedded scalable platforms, in: Proceedings of the 53rd Annual Design Automation Conference, 2016, pp. 1–6.

[41] A. Amid, D. Biancolin, A. Gonzalez, D. Grubb, S. Karandikar, H. Liew, A. Magyar, H. Mao, A. Ou, N. Pemberton, et al., Chipyard: Integrated design, simulation, and implementation framework for custom socs, IEEE Micro 40 (4) (2020) 10–21.

[42] M.H. Quraishi, E.B. Tavakoli, F. Ren, A survey of system architectures and techniques for fpga virtualization, IEEE Trans. Parallel Distrib. Syst. 32 (9) (2021) 2216–2230.

[43] A. Lambertini, E. Mandanici, M.A. Tini, L. Vittuari, Technical challenges for multi-temporal and multi-sensor image processing surveyed by UAV for mapping and monitoring in precision agriculture, Remote. Sens. 14 (19) (2022) 4954.

[44] C. Chen, Z. Zheng, T. Xu, S. Guo, S. Feng, W. Yao, Y. Lan, Yolo-based uav technology: A review of the research and its applications, Drones 7 (3) (2023) 190.

[45] A. Sassu, J. Motta, A. Deidda, L. Ghiani, A. Carlevaro, G. Garibotto, F. Gambella, Artichoke deep learning detection network for site-specific agrochemicals uas spraying, Comput. Electron. Agric. 213 (2023) 108185.

[46] F.A. Almalki, B.O. Soufiene, S.H. Alsamhi, H. Sakli, A low-cost platform for environmental smart farming monitoring system based on IoT and UAVs, Sustainability 13 (11) (2021) 5908.

[47] C. Qu, J. Boubin, D. Gafurov, J. Zhou, N. Aloysius, H. Nguyen, P. Calyam, Uav swarms in smart agriculture: Experiences and opportunities, in: 2022 IEEE 18th International Conference on E-Science (E-Science), IEEE, 2022, pp. 148–158.

[48] A.I. de Castro, Y. Shi, J.M. Maja, J.M. Peña, UAVs for vegetation monitoring: Overview and recent scientific contributions, Remote. Sens. 13 (11) (2021) 2139.

[49] A. Abbas, Z. Zhang, H. Zheng, M.M. Alami, A.F. Alrefaei, Q. Abbas, S.A.H. Naqvi, M.J. Rao, W.F. Mosa, Q. Abbas, et al., Drones in plant disease assessment, efficient monitoring, and detection: a way forward to smart agriculture, Agronomy 13 (6) (2023) 1524.

[50] N. Kitpo, M. Inoue, Early rice disease detection and position mapping system using drone and IoT architecture, SEATUC, in: 2018 12th South East Asian Technical University Consortium, Vol. 1, IEEE, 2018, pp. 1–5.

[51] J. Su, C. Liu, M. Coombes, X. Hu, C. Wang, X. Xu, Q. Li, L. Guo, W.-H. Chen, Wheat yellow rust monitoring by learning from multispectral UAV aerial imagery, Comput. Electron. Agric. 155 (2018) 157–166.

[52] T. Talaviya, D. Shah, N. Patel, H. Yagnik, M. Shah, Implementation of artificial intelligence in agriculture for optimisation of irrigation and application of pesticides and herbicides, Artif. Intell. Agric. 4 (2020) 58–73.

[53] B.S. Faiçal, H. Freitas, P.H. Gomes, L.Y. Mano, G. Pessin, A.C. de Carvalho, B. Krishnamachari, J. Ueyama, An adaptive approach for UAV-based pesticide spraying in dynamic environments, Comput. Electron. Agric. 138 (2017) 210–223.

[54] D. Debnath, F. Vanegas, J. Sandino, A.F. Hawary, F. Gonzalez, A review of UAV path-planning algorithms and obstacle avoidance methods for remote sensing applications, Remote. Sens. 16 (21) (2024) 4019.

[55] S. Ahmed, B. Qiu, F. Ahmad, C.-W. Kong, H. Xin, A state-of-the-art analysis of obstacle avoidance methods from the perspective of an agricultural sprayer UAV's operation scenario, Agronomy 11 (6) (2021) 1069.

[56] L. Wang, Y. Lan, Y. Zhang, H. Zhang, M.N. Tahir, S. Ou, X. Liu, P. Chen, Applications and prospects of agricultural unmanned aerial vehicle obstacle avoidance technology in China, Sensors 19 (3) (2019) 642.

[57] C.-L. Sotiropoulou, C. Gentsos, S. Nikolaidis, A. Rjoub, FPGA-based canny edge detection for real-time applications, in: Published At the 26th Conference on Design of Circuits and Integrated Systems, DCIS, Albufeira, Portugal, 2011.

[58] B.H.Y. Alsalam, K. Morton, D. Campbell, F. Gonzalez, Autonomous UAV with vision based on-board decision making for remote sensing and precision agriculture, in: 2017 IEEE Aerospace Conference, IEEE, 2017, pp. 1–12.

[59] B. Dai, Y. He, F. Gu, L. Yang, J. Han, W. Xu, A vision-based autonomous aerial spray system for precision agriculture, in: 2017 Ieee International Conference on Robotics and Biomimetics, ROBIO, IEEE, 2017, pp. 507–513.

[60] P. Horstrand, R. Guerra, A. Rodríguez, M. Díaz, S. López, J.F. López, A UAV platform based on a hyperspectral sensor for image capturing and on-board processing, IEEE Access 7 (2019) 66919–66938.

[61] A. Saddik, R. Latif, A. El Ouardi, Low-power FPGA architecture based monitoring applications in precision agriculture, J. Low Power Electron. Appl. 11 (4) (2021) 39.

[62] PYNQ - Python productivity for Zynq, URL http://www.pynq.io/.

[63] V. Mayoral-Vilches, S.M. Neuman, B. Plancher, V.J. Reddi, Robotcore: An open architecture for hardware acceleration in ros 2, in: 2022 IEEE/RSJ International Conference on Intelligent Robots and Systems, IROS, IEEE, 2022, pp. 9692–9699.

[64] D. Giri, K.-L. Chiu, G. Eichler, P. Mantovani, L.P. Carloni, Accelerator integration for open-source SoC design, IEEE Micro 41 (4) (2021) 8–14.

[65] C. Heinz, J. Hofmann, J. Korinth, L. Sommer, L. Weber, A. Koch, The TaPaSCo open-source toolflow: For the automated composition of task-based parallel reconfigurable computing systems, J. Signal Process. Syst. 93 (2021) 545–563.

[66] M. Bouhali, F. Shamani, Z.E. Dahmane, A. Belaidi, J. Nurmi, FPGA applications in unmanned aerial vehicles-a review, in: Applied Reconfigurable Computing: 13th International Symposium, ARC 2017, Delft, the Netherlands, April 3-7, 2017, Proceedings 13, Springer, 2017, pp. 217–228.

[67] N.H. Malle, F.F. Nyboe, E.S.M. Ebeid, Onboard powerline perception system for uavs using mmwave radar and fpga-accelerated vision, IEEE Access 10 (2022) 113543–113559.

[68] K. Guo, S. Zeng, J. Yu, Y. Wang, H. Yang, A survey of FPGA-based neural network accelerator, 2017, arXiv preprint arXiv:1712.08934.

[69] A.K. Jain, X. Li, P. Singhai, D.L. Maskell, S.A. Fahmy, DeCO: A DSP block based FPGA accelerator overlay with low overhead interconnect, in: 2016 IEEE 24th Annual International Symposium on Field-Programmable Custom Computing Machines, FCCM, IEEE, 2016, pp. 1–8.

[70] B. Hutchings, M. Wirthlin, Rapid implementation of a partially reconfigurable video system with PYNQ, in: 2017 27th International Conference on Field Programmable Logic and Applications, FPL, IEEE, 2017, pp. 1–8.

[71] The Composable Video Pipeline — PYNQ Composable Overlays 1.0.2 documentation, URL https://pynq-composable.readthedocs.io/en/latest/video_pipeline.html.

[72] J. Goeders, T. Gaskin, B. Hutchings, Demand driven assembly of fpga configurations using partial reconfiguration, ubuntu linux, and pynq, in: 2018 IEEE 26th Annual International Symposium on Field-Programmable Custom Computing Machines, FCCM, IEEE, 2018, pp. 149–156.

[73] G. Tagliavini, D. Cesarini, A. Marongiu, Unleashing fine-grained parallelism on embedded many-core accelerators with lightweight OpenMP tasking, IEEE Trans. Parallel Distrib. Syst. 29 (9) (2018) 2150–2163.

[74] A. Kurth, A. Capotondi, P. Vogel, L. Benini, A. Marongiu, HERO: An open-source research platform for HW/SW exploration of heterogeneous manycore systems, in: Proceedings of the 2nd Workshop on AutotuniNg and ADaptivity AppRoaches for Energy Efficient HPC Systems, 2018, pp. 1–6.

[75] G. Bellocchi, A. Capotondi, F. Conti, A. Marongiu, A RISC-V-based FPGA overlay to simplify embedded accelerator deployment, in: 2021 24th Euromicro Conference on Digital System Design, DSD, IEEE, 2021, pp. 9–17.

[76] D. Rossi, F. Conti, A. Marongiu, A. Pullini, I. Loi, M. Gautschi, G. Tagliavini, A. Capotondi, P. Flatresse, L. Benini, PULP: A parallel ultra low power platform for next generation IoT applications, in: 2015 IEEE Hot Chips 27 Symposium, HCS, IEEE, 2015, pp. 1–39.

[77] Zynq UltraScale+ MPSoC, URL https://www.xilinx.com/products/silicon-devices/soc/zynq-ultrascale-mpsoc.html.

[78] V. Boppana, S. Ahmad, I. Ganusov, V. Kathail, V. Rajagopalan, R. Wittig, UltraScale+ MPSoC and FPGA families, in: 2015 IEEE Hot Chips 27 Symposium, HCS, IEEE, 2015, pp. 1–37.

[79] F. Zaruba, L. Benini, The cost of application-class processing: Energy and performance analysis of a Linux-ready 1.7-GHz 64-bit RISC-V core in 22-nm FDSOI technology, IEEE Trans. Very Large Scale Integr. (VLSI) Syst. 27 (11) (2019-11) 2629–2640, http://dx.doi.org/10.1109/TVLSI.2019.2926114.

[80] A. Bernardi, G. Brilli, A. Capotondi, A. Marongiu, P. Burgio, An FPGA overlay for efficient real-time localization in 1/10th scale autonomous vehicles, in: 2022 Design, Automation & Test in Europe Conference & Exhibition, DATE, IEEE, 2022, pp. 915–920.

[81] G. Valente, G. Brilli, T. Di Mascio, A. Capotondi, P. Burgio, P. Valente, A. Marongiu, Fine-grained QoS control via tightly-coupled bandwidth monitoring and regulation for FPGA-based heterogeneous SoCs, IEEE Trans. Parallel Distrib. Syst. (2024).

[82] P.D. Schiavone, F. Conti, D. Rossi, M. Gautschi, A. Pullini, E. Flamand, L. Benini, Slow and steady wins the race? A comparison of ultra-low-power RISC-V cores for Internet-of-Things applications, in: 2017 27th International Symposium on Power and Timing Modeling, Optimization and Simulation, PATMOS, IEEE, 2017, pp. 1–8.

[83] M. Gautschi, P.D. Schiavone, A. Traber, I. Loi, A. Pullini, D. Rossi, E. Flamand, F.K. Gürkaynak, L. Benini, Near-threshold RISC-V core with DSP extensions for scalable IoT endpoint devices, IEEE Trans. Very Large Scale Integr. (VLSI) Syst. 25 (10) (2017-10) 2700–2713, http://dx.doi.org/10.1109/TVLSI.2017.2654506.

[84] F. Conti, L. Benini, A ultra-low-energy convolution engine for fast brain-inspired vision in multicore clusters, in: 2015 Design, Automation Test in Europe Conference Exhibition, DATE, 2015-03, pp. 683–688, http://dx.doi.org/10.7873/DATE.2015.0404, ISSN: 1558-1101.

[85] F. Conti, P.D. Schiavone, L. Benini, XNOR neural engine: A hardware accelerator IP for 21.6-fJ/op binary neural network inference, IEEE Trans. Comput.-Aided Des. Integr. Circuits Syst. 37 (11) (2018-11) 2940–2951, http://dx.doi.org/10.1109/TCAD.2018.2857019.

[86] C. Sau, T. Fanni, C. Rubattu, L. Raffo, F. Palumbo, The multi-dataflow composer tool: An open-source tool suite for optimized coarse-grain reconfigurable hardware accelerators and platform design, Microprocess. Microsyst. 80 (2021) 103326.

[87] T. Fanni, A. Rodríguez, C. Sau, L. Suriano, F. Palumbo, L. Raffo, E. de la Torre, Multi-grain reconfiguration for advanced adaptivity in cyber-physical systems, in: 2018 International Conference on ReConFigurable Computing and FPGAs, ReConFig, IEEE, 2018, pp. 1–8.

[88] J. Sérot, F. Berry, S. Ahmed, CAPH: a language for implementing stream-processing applications on FPGAs, in: Embedded Systems Design with FPGAs, Springer, 2013, pp. 201–224.

[89] E. Flamand, D. Rossi, F. Conti, I. Loi, A. Pullini, F. Rotenberg, L. Benini, GAP-8: A RISC-V SoC for AI at the edge of the IoT, in: 2018 IEEE 29th International Conference on Application-Specific Systems, Architectures and Processors, ASAP, IEEE, 2018, pp. 1–4.

[90] B.D. De Dinechin, R. Ayrignac, P.-E. Beaucamps, P. Couvert, B. Ganne, P.G. de Massas, F. Jacquet, S. Jones, N.M. Chaisemartin, F. Riss, et al., A clustered manycore processor architecture for embedded and accelerated applications, in: 2013 IEEE High Performance Extreme Computing Conference, HPEC, IEEE, 2013, pp. 1–6.

[91] E. Lindholm, J. Nickolls, S. Oberman, J. Montrym, NVIDIA Tesla: A unified graphics and computing architecture, IEEE Micro 28 (2) (2008) 39–55.

[92] T. Fischer, M. Rogenmoser, T. Benz, F.K. Gürkaynak, L. Benini, FlooNoC: A 645-Gb/s/link 0.15-pJ/B/hop open-source NoC with wide physical links and end-to-end AXI4 parallel multistream support, IEEE Trans. Very Large Scale Integr. (VLSI) Syst. (2025).

[93] Y. Lei, Q. Deng, S. Long, S. Liu, S. Oh, An effective design to improve the efficiency of DPUs on FPGA, in: 2020 IEEE 26th International Conference on Parallel and Distributed Systems, ICPADS, IEEE, 2020, pp. 206–213.

[94] A. Magnani, G. Brilli, A. Marongiu, Architectural design exploration of a lane detection vision pipeline for FPGA-based F1tenth autonomous vehicles, in: Proceedings of the 22nd ACM International Conference on Computing Frontiers: Workshops and Special Sessions, 2025, pp. 46–49.

[95] G. Bellocchi, A. Capotondi, L. Benini, A. Marongiu, Enabling fast system-level integration and prototyping of accelerator-rich platforms, in: Proceedings of the 22nd ACM International Conference on Computing Frontiers: Workshops and Special Sessions, 2025, pp. 54–57.

[96] M. O'Kelly, H. Zheng, D. Karthik, R. Mangharam, F1tenth: An open-source evaluation environment for continuous control and reinforcement learning, Proc. Mach. Learn. Res. 123 (2020).

[97] Vitis Libraries, URL https://www.xilinx.com/products/design-tools/vitis/vitis-libraries.html.

Gianluca Bellocchi received his B.Sc. and M.Sc. degrees in Electronic Engineering from the University of Modena and Reggio Emilia. He is currently pursuing a Ph.D. under Prof. Marongiu at the same university. He was an academic guest at ETH Zürich, Switzerland, and an exchange student at Mittuniversitetet, Sweden. His research interests include real-time, predictable on-chip interconnects, hardware-software co-design of heterogeneous systems-on-chip, and system-level design methodologies.

Daniel Madroñal received his Ph.D. (cum laude) at Universidad Politécnica de Madrid in 2020, defending the thesis entitled "Energy Consumption Reduction on High Performance Embedded Systems for Hyperspectral Imaging Cancer Detection". He is currently a postdoctoral researcher at the University of Sassari, where his research focuses on code generation tools to automate the design for advanced reconfigurable hardware architectures using dataflow approaches. At the moment, his work revolves around the field of companion computers to perform real-time onboard processing on UAVs and UGVs employed in the context of smart and precision agriculture.

Alessandro Capotondi (Member, IEEE) is Assistant Professor at the University of Modena and Reggio Emilia. He received his Ph.D. in Computer and Electronic Engineering from the University of Bologna. His research interests focus mainly on HW/SW codesign of embedded systems and heterogeneous computing. In these areas, he has published more than 30 papers in international peer-reviewed conferences and journals, with over 1000 citations and an h-index of 15 [Google Scholar].

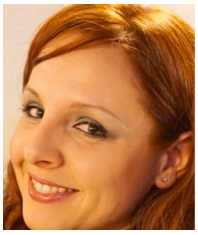

Francesca Palumbo is an Associate Professor at the University of Cagliari. Her primary research focus is on embedded, cyberphysical, and reconfigurable systems, as well as code generation tools and design automation strategies for advanced reconfigurable hardware architectures. She has over 80 Scopus indexed publications on refereed international journals and conference proceedings. In addition, she has served in over 60 Technical Committees of international conferences and organized more than 20 different international conferences/schools, covering roles such as Program Chair and once General Chair. She is a member of HiPEAC, has been elevated to the Senior Grade within IEEE, and is a member of ACM and the SIE (Italian Society of Electronics). She is also a permanent Steering Committee Member of the ACM Conference on Computing Frontiers and Associate Editor of the IEEE Embedded Systems Letters and the Springer Journal of Signal Processing Systems. In 2018, she joined the IEEE VLSI Systems Applications Technical Committee (VSA-TC). Currently, she is participating in different EU projects, and she is the Scientific Coordinator of the MYRTUS project on cognitive continuum computing technologies. Finally, since 2017, she has been the Director of the CPS Summer School "Designing Cyber-Physical Systems – From concepts to implementation," now at its sixth edition.

Andrea Marongiu (Member, IEEE) received his Ph.D. in Computer and Electronic Engineering from the University of Bologna, Italy, in 2010. He has been a postdoctoral research fellow at ETH Zürich, Switzerland. He is currently an associate professor at the University of Modena and Reggio Emilia. His research interests focus on programming models and architectures for heterogeneous multi- and many-core systems-on-chip. In this field, he has published more than 120 papers in peer-reviewed conferences and journals.